Fuel 364 (2024) 131063

Contents lists available at ScienceDirect

Fuel

journal homepage: www.elsevier.com/locate/fuel

Full Length Article

Crude oil cracking under geological conditions: A case study of the Ediacaran reservoir, central Sichuan Basin, China

Yishu Li [a,b], Guangdi Liu [a,b,*], Zezhang Song [a,b,*], Mingliang Sun [a,b], Xingwang Tian [c], Dailing Yang [c], Lianqiang Zhu [a,b]

[a] State Key Laboratory of Petroleum Resources and Prospecting, China University of Petroleum, Beijing 102249, China
[b] College of Geosciences, China University of Petroleum, Beijing 102249, China
[c] Exploration and Development Research Institute of Southwest Oil & Gas Field Company, PetroChina, Chengdu 610041, China

ARTICLE INFO

Keywords:
Oil cracking
Kinetic model
Thermal stability
U–Pb dating
Geological conditions
Ediacaran reservoir

ABSTRACT

Deep strata are extremely rich in hydrocarbon resources, and trap oil has undergone a long-term and multistage geological evolution that results in thermal cracking. However, compared with controlled experimental conditions, studies on the thermal cracking process of trapped oil under subsurface geological conditions are relatively scarce. Therefore, the major aim of this study is to reconstruct the oil reservoir cracking process based on an evolutionary study of a typical Ediacaran gas reservoir in China. By evaluating the detailed reservoir petrology, natural gas composition, isotopes, residual solid bitumen (SB) characteristics, fluid inclusion analysis, and in situ U–Pb dating of dolomite, this study combined an oil cracking kinetic model with actual geological elements and evolution to recover the four stages of trap oil cracking. Mutual verification of the forward model and inversion demonstrated that a suitable oil cracking kinetic model can be extrapolated to geological conditions. With an increase in the thermal evolution of the reservoir, the most unstable component in the oil first cracks, and a small amount of gaseous products are preferentially dissolved in the liquid oil. The major components of petroleum undergo thermal cracking and conversion to produce short-chain liquid hydrocarbons and wet gases. A large amount of wet gas generates an abnormally high fluid pressure. Wet gas usually escapes from potential channels (i.e., caprock microfractures and unconformity surfaces), thus dynamically maintaining the energy balance of the trap system and weakening the impact of high pressure on oil cracking. The wet gas products precipitate asphaltene in the oil, thus adjusting the composition and properties of the trap oil. The escape of the initial wet gas products, accompanied by a thermochemical sulfate reduction (TSR) reaction with residual oil, C_2H_6, and other wet gases as reactants, led to the formation of CH_4-rich natural gas with a high drying coefficient in the trap of the highly over-mature evolution stage. Precipitated asphalt and the asphalt directly produced by oil cracking, coke rapidly under high temperatures and pressures to form SB with abnormally high reflectivity. Under geological conditions, oil cracking behavior is generally controlled by a combination of temperature history, tectonic history, fluid pressure background, trap preservation conditions, secondary alteration (e.g., TSR), and oil type, among which the reservoir temperature history remains the most important. Other factors should not be underestimated in a specific region. This study revealed a pathway model for the thermal cracking of trapped oil under real geological conditions, providing references for similar studies and other pathway models in different regions worldwide.

1. Introduction

Natural gas is an important source of fossil fuels and accounts for the highest proportion of the energy structure because it is cleaner than coal and oil. Gas produced by crude oil cracking is a special natural gas source discovered in the deep-ultra-deep layers of several basins worldwide [1–7]. Under the control of temperature and heating time (T–t), organic-rich source rocks will reach the critical value of hydrocarbon generation and expulsion [8]. The oil and gas properties during this period largely depend on the source rock characteristics (e.g., organic matter type and paleoenvironment) [9]. When hydrocarbons migrate into traps, secondary changes may occur (e.g., thermal

* Corresponding authors at: State Key Laboratory of Petroleum Resources and Prospecting, China University of Petroleum, Beijing 102249, China.
E-mail addresses: lgd@cup.edu.cn (G. Liu), songzz@cup.edu.cn (Z. Song).

https://doi.org/10.1016/j.fuel.2024.131063
Received 16 March 2023; Received in revised form 3 January 2024; Accepted 21 January 2024
Available online 28 January 2024

maturation, deasphalting, and biodegradation) [9–11]. Crude oil cracking is an important component of the hydrocarbon generation theory for kerogen. Driven by T–t, the degree of thermal evolution increases, and the C–C bonds of macromolecular hydrocarbons in oil gradually break, forming low-molecular-weight hydrocarbons. When this disproportionation reaction occurs, the crude oil composition changed significantly [8]. The degradation of long-chain molecules generally forms light hydrocarbon [12,13], leading to the consumption of polycyclic biomarkers and an increase in the gas-oil ratio [9]. Only the most thermodynamically stable gases (predominantly methane, CH_4) and residual coke solid bitumen (SB) remain in the reservoir [10,14,15]. This process conforms to chemical kinetics, and most researchers have summarized it as follows: breaking of strong electronegative bonds (including C–O and C–S bonds), such as asphaltenes in the composite components; cracking of saturated hydrocarbons > C_6; demethylation, i.e., cracking of aromatics to produce low-molecular-weight saturated hydrocarbons and coke; and further cracking of small molecular hydrocarbons ($C_{3–5}$). Thermal simulations of oil based on an autoclave, a micro-sealed container, and a gold tube have revealed this process [2,12,13,15–19].

Currently, the Ediacaran Dengying (DY) Formation in the central Sichuan Basin is buried at a depth of approximately 5500 m and a temperature of 160 °C, but the reservoir is filled with dry gas (dry coefficient > 0.99) and coke SB [4]. The lower limits of oil thermal stability in the diverse study areas are different, and the lower limit of liquid oil obtained by a constant heating path (2–5 °C/Ma) based on laboratory conditions is not constant and is predominantly related to the T–t evolution conditions of the actual reservoir. In addition, several studies have demonstrated that oil composition and properties, fluid pressure conditions, reservoir mineral types, thermochemical sulfate reduction (TSR) reactions, and mixing effects promote or inhibit the oil cracking process to a certain extent [13,18–26]. The Ediacaran DY Formation gas reservoir in the central Sichuan Basin has been formed by in-situ oil cracking, the final stage of cracking, and has undergone complete thermal cracking process [4,7,27]. Owing to the complex geological evolution of deep-buried carbonate reservoirs, which generally experience multiple uplifts and subsidence (tectonic events), it is challenging to describe and restore their fluid-filling history and oil and gas evolution. How the oil reservoir of the DY Formation in the central Sichuan Basin is thermally cracked into a gas reservoir has not yet been studied; this provides an ideal place for us to investigate the thermal stability and cracking process of crude oil under geological conditions.

Fluid inclusions are mineral thermometers that record the evolution of the original fluid in a reservoir. Several advances have been made in the study of fluid inclusions, including the determination of single components, homogenization temperature (Th) recovery, and paleopressure systems. These have become essential for studying the fluid-phase state during multistage evolution and recovery [28]. Additionally, dating technology for carbonate minerals, particularly low-uranium dolomite, has been greatly developed [29], providing key information for mineralogical verification, and thus improving the accuracy of oil cracking research. Although the kinetic activation energy (E) transformation under laboratory conditions may not always be completely applicable under geological conditions, it has been widely used in relevant research and has become an important tool for evaluating the oil cracking process [13,18,19,21,23,26,30].

In this study, based on the study of reservoir petrology, we have accurately dated the key minerals. Along with the reservoir P–T evolution and recovery during geological history, kinetic optimization simulations, and mutual verification of fluid inclusions, the complete evolution process of crude oil after entering the reservoir was reconstructed and constrained to emphasize the thermal stability of crude oil under real or near-real geological formation conditions. This study not only considered the oil thermal stability under the actual geological conditions of the basin, but also provided confidence for the resource potential of deeper basins under specific geological conditions. Therefore, studying the oil preservation and cracking processes under geological conditions is of theoretical significance. This study also serves as a reference for subsequent studies conducted in diverse regions.

2. Geological setting

The Sichuan Basin is rhombic and surrounded by a series of mountains (Fig. 1a). The surface elevation of the central Sichuan Basin is approximately 250–650 m and the terrain is flat (Fig. 1b). The top depth of the Ediacaran DY Formation can reach 4800–9000 m, and comprises two adjacent tectonic units: the Gaoshiti–Moxi (GM) and North Slope (NS). The anticline structure, with the GM area as the core of the uplift, gradually transformed into a vast and gentle monocline structure in the NS area (Fig. 1c). This uplift is old, inherited, and has a high structural location in the central Sichuan Basin as well as a favorable location for reservoir accumulation. The NS area is an epigenetic monoclinic structure predominantly formed by enhancing the amplitude of the Indian Yanshanian monoclinic structure. Recently, large lithological gas reservoirs have been identified [27]. The DY Formation is divided into four parts (Fig. 1d), of which DY2 and DY4 are gas distribution layers (Fig. 1e), mainly dolomite. The reservoir is a mound beach facies and karst composite formation. Several studies have been conducted on the origin of the cracked gas in this reservoir, including the compositional relationship between methane (CH_4), ethane (C_2H_6), and propane (C_3H_8); the relationship between isoalkanes and cycloalkanes in light hydrocarbons; and an inclusion-based cracking model [4,7,31]. The source rock is a paleo-oil reservoir with several contributing factors, including the Cambrian Qiongzhusi, DY, and Doushantuo Formations. The Qiongzhusi Formation is comprised of thick black shale with small amounts of argillaceous silt and dolomite at the top. The thicknesses of these source rocks can reach 150–700 m, and the average organic matter content is > 2.5 %. Additionally, the mud shales of the DY3 and Doushantuo Formations are relatively thin, at approximately 30–40 m and 10–30 m, respectively, which is conducive to the formation of oil reservoirs. The DY Formation contains structural configurations of high-quality oil and gas reservoirs. A large amount of oil migrated laterally from the Deyang-Anyue rift trough and mixed with oil generated in situ from source rocks in the GM and NS areas. The direct caprock at the top was also a source rock with good preservation conditions.

3. Samples and methods

We systematically observed the DY Formation reservoir cores from seven wells and obtained over 50 samples. For typical samples, conventional blue epoxy resin cast (0.05 mm), cathodoluminescent (CL) (0.03 mm), and inclusion thin sections (0.01 mm), and fresh natural section samples of approximately 1 cm^3 with weathered surfaces removed were prepared, and transmission light, CL, and scanning electron microscopy (SEM) observations were conducted. Additionally, inclusion analysis was conducted on 10 samples, organic element analysis on 11 SB samples, in-situ dolomite U–Pb dating on two samples, and basin simulation analysis on 15 wells.

3.1. Thin section and SEM observation

The transmitted light was observed using a Leica 4500P microscope, and the CL was observed on a CL8200–MK5 CL instrument. At room temperature of approximately 25 °C, the CL instrument chamber was vacuumed to produce an electron beam with approximately 8–25 kV voltage and 0.1–1.0 mA current, which produced diverse luminous colors when interacting with minerals. Fresh natural cross-sectional samples were coated with gold to enhance their electrical conductivity and were observed using a Quanta 200F SEM and an energy dispersive X-ray spectrometer to quantify the elemental content of the target minerals.

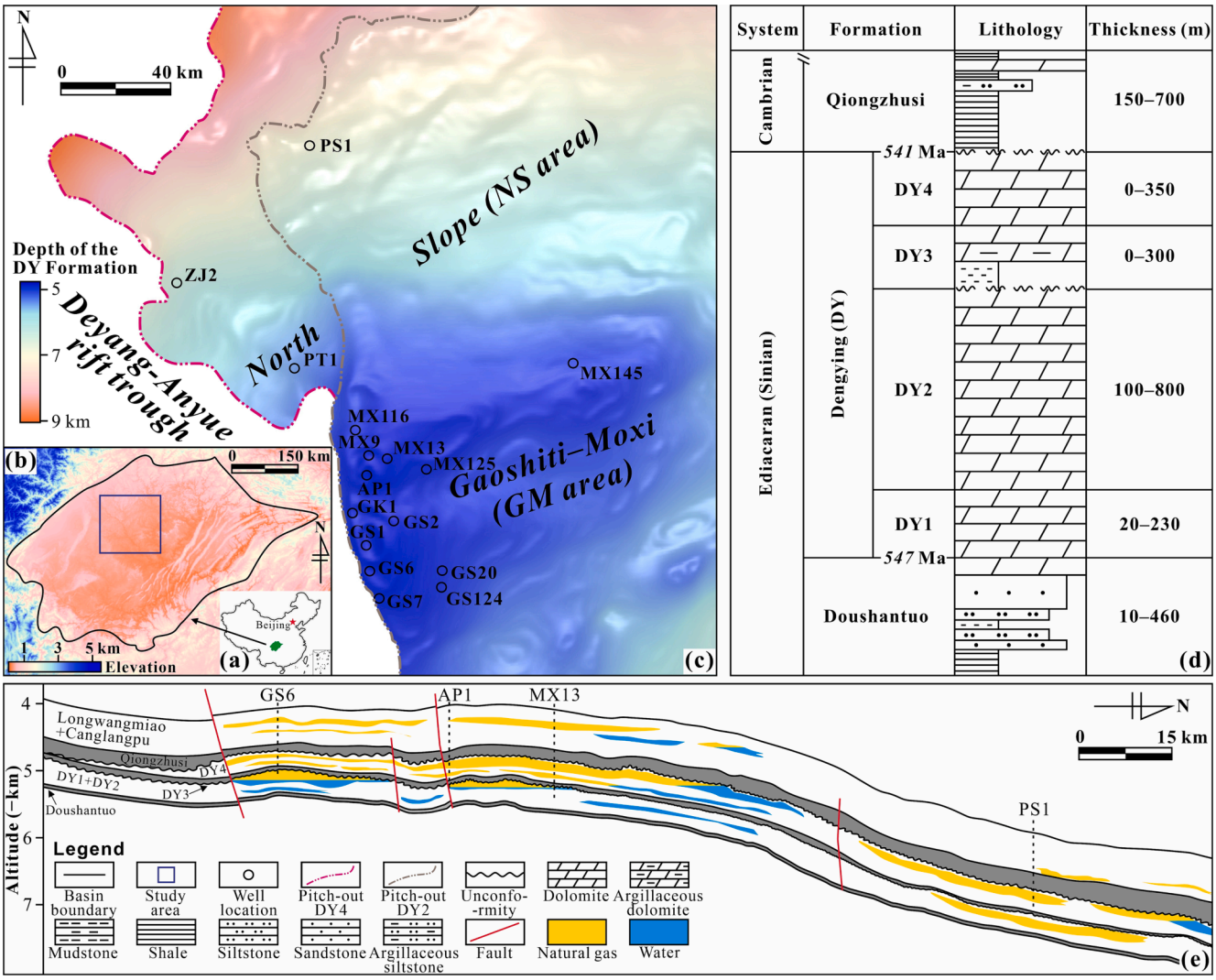

Fig. 1. A comprehensive geological overview of the study area. (a) Geographic location and (b) topography of the Sichuan Basin and the location of the study area; (c) structural map, (d) stratigraphic histogram, and (e) natural gas reservoir section of the Dengying (DY) Formation in the central Sichuan Basin.

3.2. Fluid inclusion tests

Fluid inclusions were observed under a Leica DM2500P microscope and tested on a LINKAM THMS600 cooling-heating stage coupled to a microscope. The Th of the liquid and gaseous inclusions were measured using a heating rate of 10 °C/min below 60 °C and 5 °C/min above 60 °C with an accuracy of ± 1 °C. Additionally, a LabHR-VIS LabRAM HR800 research-grade microlaser Raman spectrometer equipped with a Yag crystal frequency-doubled solid-state laser was used to evaluate the composition of the inclusions with a scanning range of 100–4200 cm^{-1}. The capture fluid pressure of pure-CH_4 inclusions was based on the Raman spectrum shift. By comparing the CH_4 displacement with the standard sample, the density of the pure-CH_4 inclusion was calculated [32,33], and its pressure was calculated based on the density and Th [34]. The analysis was conducted at the Beijing Research Institute of Uranium Geology, China.

3.3. U–Pb dating

U–Pb dating of dolomite was conducted using laser-ablation-inductively coupled plasma-mass spectrometry (LA-ICP-MS) technique, where the systematically observed slices were cleaned in an ultrasonic cleaning apparatus with deionized water for 4 h and then dried at 50 °C. A resolution LR 193 nm ArF laser denudation system and a highly sensitive collector (Thermo Fisher iCap-TQ, ICP-MS) were used to obtain the U–Pb isotopes of the minerals. The $^{207}Pb/^{206}Pb$ values of the standard samples were corrected using the NIST 614. The $^{238}U/^{206}Pb$ values of sub-standard PTKD-2 (153.7 ± 1.7 Ma) and the sample were corrected with primary standard AHX-1d (238.2 ± 0.9 Ma), and the U–Pb isotope ratios were treated with Iolite software [35]. Detailed experimental procedures are described by Cheng et al. [29].

3.4. Organic element test

SB was powdered in an agate mortar and tested for elemental C, H, N, and O using an elemental cube analyzer. Elemental C, H, and N were obtained by combustion under O and the detection of CO_2, H_2O, and N_2 products, while element O was tested separately and calculated using the CO products of high-temperature pyrolysis.

3.5. Kinetic modelling

Basin modeling is widely used to quantify burial paths, P–T and thermal evolution, and hydrocarbon generation and expulsion processes. Based on the PetroMod software combined with the lithology, geological stratification, thickness, and denudation events of the current strata in the study area, the burial history of the DY Formation of the 15 wells was restored. The formation lithology, stratification, and thickness

were derived from well completion and production test reports of the PetroChina Southwest Oil and Gas Field. Denudation events were defined based on the published research results. Based on the geothermal flow history of the study area, the DY Formation temperature and hydrostatic pressure evolution were restored using the published measured maturity data, measured borehole temperature, and pressure calibration in the oilfield. The supporting kinetic data for petroleum cracking obtained from the previously published literature were classified according to the experimental conditions and then simulated according to the actual geological and thermal history of the reservoir.

4. Results and discussion

4.1. Petrological characteristics and dating of dolomite

In the DY Formation reservoir, there are two major types of dolomite far from the host rock (HR) (near the pore center). The first was fine-crystal dolomite (Dol–1), which had fine particles, irregular shapes, and other crystals, and was chaotic and dark under transmitted light. Dol–1 was adjacent to the HR and was formed later. The mineral with the highest content was medium-coarse crystalline dolomite (Dol–2), which had large particles, milky white, and regular rhombic shapes,

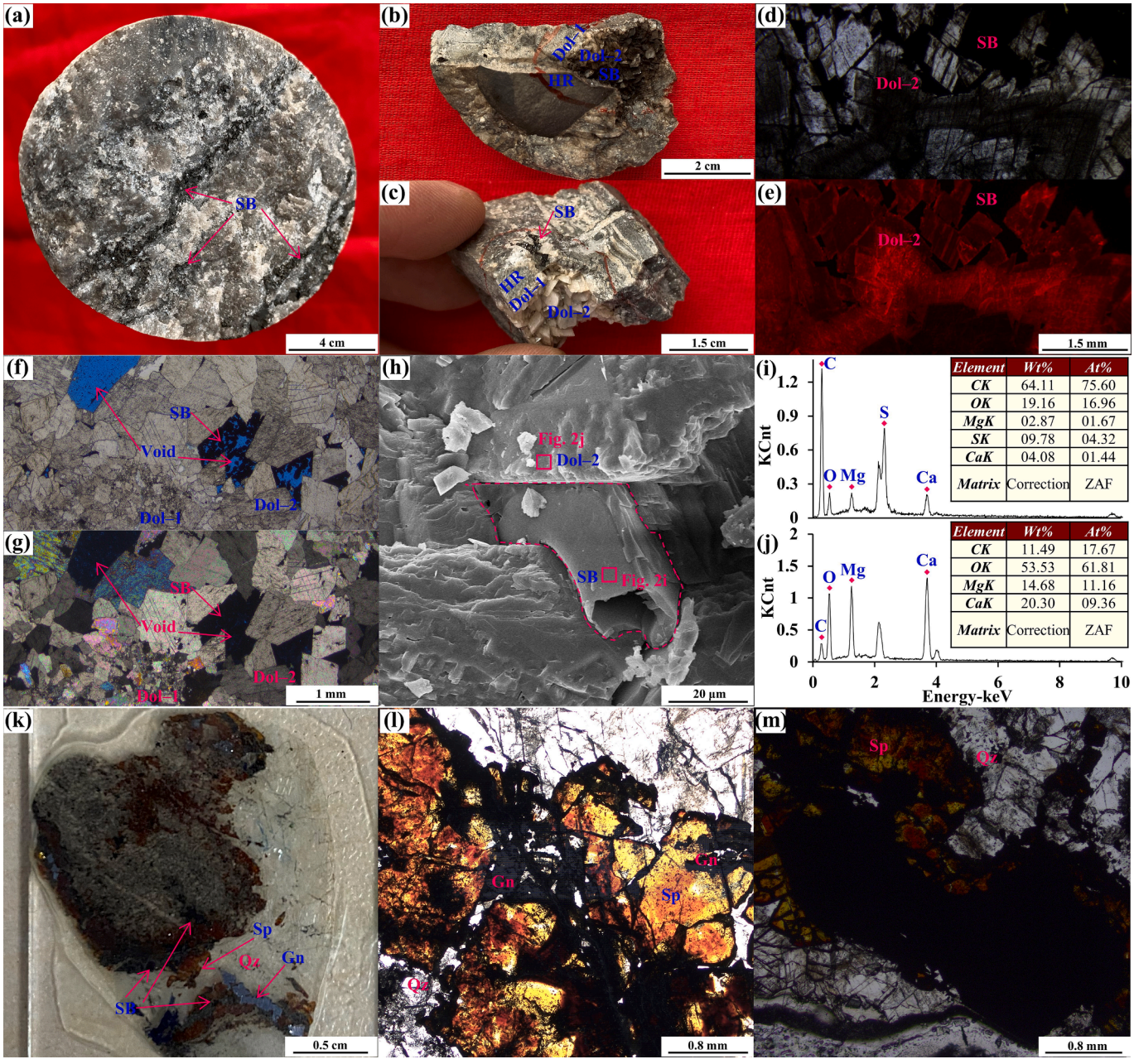

Fig. 2. Petrology and fluid inclusion characteristics of the DY Formation, central Sichuan Basin. (a) Black reservoir solid bitumen (SB) is vastly developed, PS1, 7273.87 m; (b–c) host rock (HR), early fine-grained dolomite (Dol–1), late medium-coarse grained dolomite (Dol–2) and SB are developed successively, PT1, 5779.64 m (b) and 5778.71 m (c); (d–e) plane-polarized light and CL depict bright red Dol–2, with SB formation later than Dol–2, GS20, 5183.47 m; (f–g) plane-polarized and crossed-polarized lights depict SB filling in residual pores, and the blue area is the residual void casting, PT1, 5777.24 m; (h–j) scanning electron microscopy (SEM) depicts that Dol–2 is formed earlier than SB as the SB is entirely filled along the regular edge of Dol–2, GS20, 5194.33 m. (k–m) Sphalerite (Sp) and galena (Gn) are associated with SB and quartz (Qz), GS7, 5293.16 m. (For interpretation of the references to color in this figure legend, the reader is referred to the web version of this article.)

some of which were accompanied by sickle- and saddle-textured fabrics and were highly self-crystalline (Fig. 2a–g). CL is an important method for evaluating carbonate minerals, and the luminescence color was generally related to the manganese and iron contents. Dol–2 was bright red under cathodoluminescence, with alternating light and dark stripes on the grain edge, and wavy extinction under transmitted light.

The SB formed by a large amount of cracking was black and opaque, existed between Dol–2 and the remaining pores, and was widely distributed and abundant in the DY Formation reservoir. Many SB were observed in the Weiyuan-Ziyang area to east of the Deyang-Anyue rift trough, the GM and NS areas, and the Langzhong area in the northern Sichuan Basin. Specifically, they were closely related to the paleo-structure and superimposed zone of the platform margin of the DY Formation. Its formation time was later than that of Dol–2, which was reflected in the contact relationship between the two. A large amount of SB was attached to the dolomite mineral surface (Fig. 2a–g). The microscopic scale of the SEM images also demonstrated that the SB occurred between Dol–2 with regular flat edges and did not change the Dol–2 formation direction or space (Fig. 2h–j). Currently, unfilled pores and fractures were spaces for natural gas storage. In addition, small amounts of metal sulfides such as sphalerite and galena were observed in a small number of samples associated with SB, Dol–2, and quartz (Fig. 2k–m). Therefore, Dol–1 → Dol–2 → SB could be obtained by studying the mineral facies closely related to reservoir oil and gas evolution. SB is the product of the thermal cracking of liquid oil in the reservoir; therefore, the formation time of the large-scale paleo-liquid oil reservoir and its later thermal cracking time should be later than the Dol–2 formation time.

The average U and Pb concentrations in Dol–1 were approximately 0.0309 and 0.0313 ppm, respectively, whereas those in Dol–2 were approximately 0.0179 and 0.0263 ppm, respectively (Table S1), indicating that they were low-U minerals. However, useful information can still be obtained by LA-ICP-MS. The lower focus of the Tera–Wasserburg consistency map and the mineral isochron (n = 79/99) represent the dolomite crystallization age. The Dol–1 age was 498 ± 11 Ma, and that of Dol–2 was 273 ± 24 Ma (Fig. 3). Compared with Dol–1, Dol–2 had a lower U content, which resulted in a higher MSWD and age error range; however, its age also had a certain reference value. This also indicates that large-scale oil filling, including subsequent cracking, must have occurred after 273 ± 24 Ma.

4.2. Restoration of reservoir P–T history

According to organic kerogen hydrocarbon generation theory, the thermal history of a reservoir is critical for the phase evolution of liquid oil. Central Sichuan Basin has a unique thermal history with a heat flow of approximately 53.8 mW/m^2 [36]. In geological history (Permian–-Triassic), the heat flow value peaked at ca. 259 Ma (exceeding 75–80 mW/m^2) and then gradually decreased. This is attributed to a combination of the Emeishan mantle plume and crustal extension [36]. The central Sichuan Basin is located in the outer zone of the Emeishan Basalts. Except for well ZJ2 on the west side with 46 m Permian volcanic rocks, no volcanic rocks were displayed in the other wells, indicating that the erupting lava of the Emeishan Basalt only spread to well ZJ2 and did not reach other locations in the NS and GM areas. Accordingly, after the reservoir temperature briefly reached or exceeded 250 °C due to hydrothermal intrusion (260.55 ± 0.07 ~ 257.22 ± 0.37 Ma, [37]) [38], the small amount of oil accumulated in the trap at that time may also be cracked [39], but the formation of large-scale oil reservoirs occurred after the Late Permian hydrothermal intrusion [31,40,41]. Subsequently, the reservoir temperature returned to the normal burial evolution path and gradually increased. Notably, the study area began to settle rapidly during the Middle Jurassic, reaching its maximum burial depth (with a deposition rate of approximately 40 m/Ma). As a result, the temperature in the Middle Cretaceous also increased to 220–250 °C, and the reservoir temperature in the deeply buried NS area may even exceeded 250 °C, reaching 280 °C. Subsequently, the uplift of the basin reduced the average current temperature to approximately 150 °C (Fig. 4a). This reservoir temperature history led to high-temperature thermal cracking of the trap oil in the reservoir. The detailed kinetic studies were discussed in Section 4.3.

The evolution of the reservoir fluid pressure is related to the tectonic and fluid activity histories. The deep burial of the formation led to a rapid increase in the hydrostatic pressure in the Middle Permian, and the increase in the hydrostatic pressure from the Triassic to Middle Cretaceous was the largest at approximately 72–96 MPa (Fig. 4b). Unlike hydrostatic pressure, pore fluid pressure is related to the volume of the effective reservoir space. The fluid pressure is controlled by the trap preservation capacity after oil thermal cracking. If sufficient space exists in a completely isolated system, one unit of oil cracking gas can exceed 500 volumes [42]. Liu et al. [43] used the PVTsim software to restore the DY Formation reservoir fluid pressure based on the Th, gas–liquid ratio, and gas reservoir composition of the inclusions. With the rapid subsidence of the structure and the generation of cracked gas, the fluid pressure appeared in an overpressure stage after approximately 200 Ma, and the formation pressure coefficient (fluid pressure/hydrostatic pressure) at the major stage of cracked gas was approximately 1.32–1.79, which was also verified and revealed by the study of the laser Raman shift method based on the inclusions (Fig. 4c–d). However, in the context of late tectonic uplift and pressure release caused by

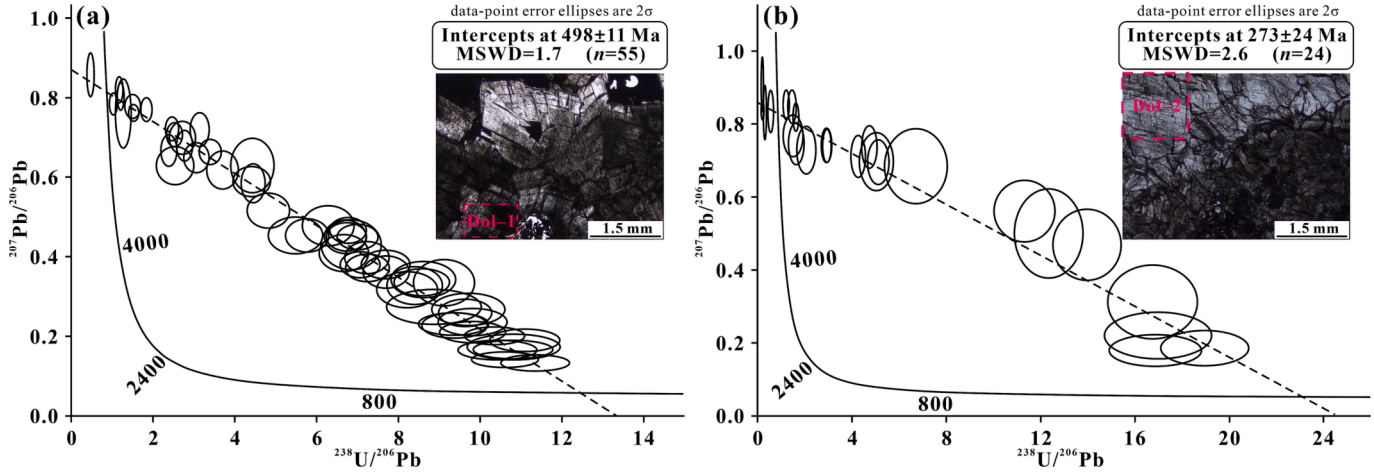

Fig. 3. Tera–Wasserburg concordia plots depicting $^{238}U/^{206}U$ versus $^{207}Pb/^{206}Pb$ for (a) Dol–1 (GS20, 5183.47 m) and (b) Dol–2 (PT1, 5779.64 m) of the DY Formation, central Sichuan Basin.

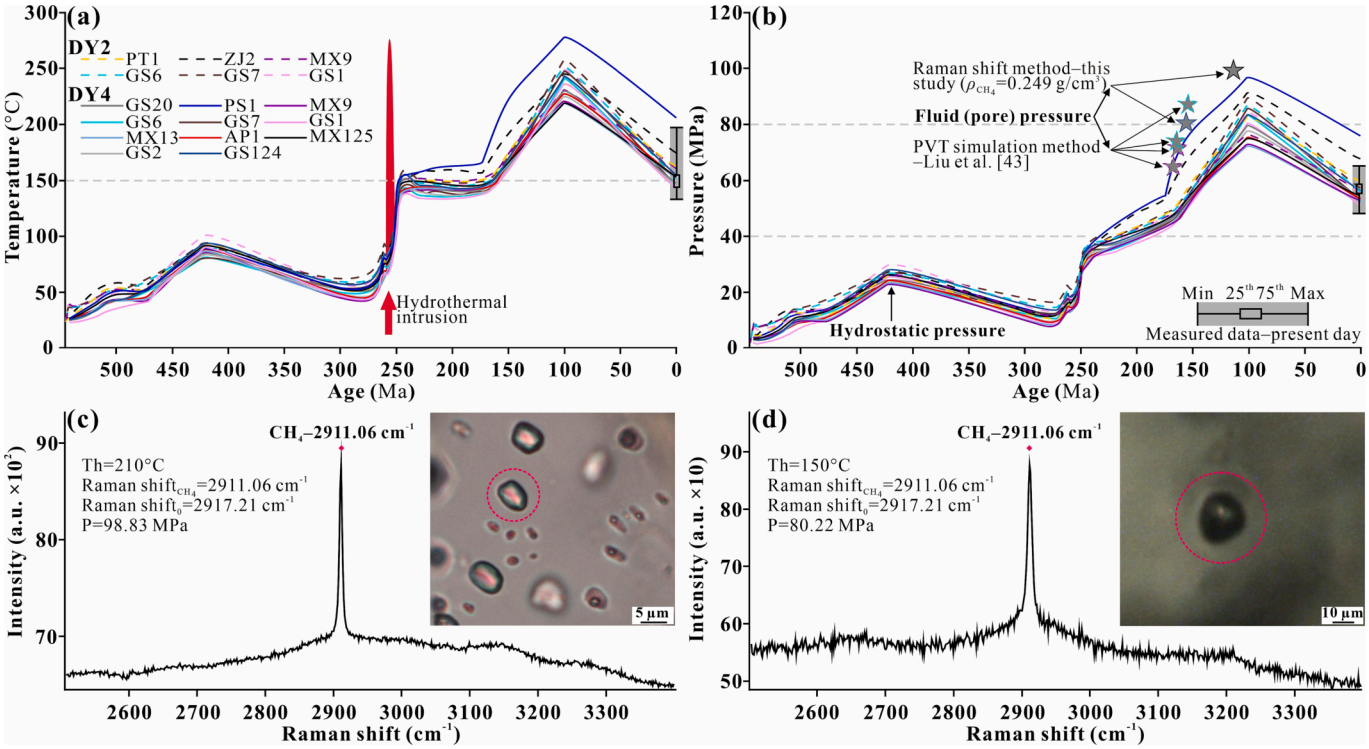

Fig. 4. Temperature (a) and pressure (b) evolution of the DY Formation, central Sichuan Basin. The lines represent the temperature and hydrostatic pressure in the middle of the DY Formation. (c–d) Two fluid pressure data (solid star shape) were obtained from Raman spectrum shift (MX125, 5385 m; GS124, 5571 m). Four fluid pressure data (dotted star shape) obtained by inclusion PVT simulation were from Liu et al. [43]. (MX9, 5427.76 m and 5445.54 m; GS6, 5365.10 m and 5380.10 m).

microfractures and unconformities in the top-cap rock, the current formation pressure of the reservoir was reduced and maintained at a normal level. As a result, the average fluid pressure of the gas reservoir was approximately 53.86 MPa, and the pressure coefficient was 1.0–1.2 (Fig. 4b).

4.3. Optimized kinetic simulation

4.3.1. Properties of trap oil

The trapped oil cracking process is similar to the source rock hydrocarbon generation process and exhibits the characteristics of a T–t complementary dynamic reaction. The rate constant (k) of the reaction was obtained using the Arrhenius equation: k = Aexp ((–E)/RT). Where A is the reaction frequency factor, R is 8.314 J/(mol·k), T is the temperature, and E is the activation energy. It is generally believed that when the oil cracking conversion rate is 51–62.5 %, the gas-oil ratio in the reservoir will exceed 23923.50–37380.46 m^3/m^3, i.e., the independent liquid reservoir will disappear [44–46]. The essence of the influence of the type of oil base material on the oil cracking process was that the content ratios of the diverse components in diverse oil systems differed, and the thermal stability of the components and compounds differed significantly.

In the same series of experiments, the dominant frequency E of heavy oil cracking gas (59 kcal/mol) was lower than those of normal (61 kcal/mol) and highly waxy oils (60 kcal/mol) [47]. Compared with lacustrine and fluviodeltaic oils, normal marine oil has a lower E and slightly poorer thermal stability [48], which seems to be predominantly due to the relatively high saturated hydrocarbon content in light oil and the formation of many aromatic compounds during gas generation. This is also proved by the pyrolysis experiments of Boscan oil (Venezuelan aromatic oil) and Pematang (Indonesian paraffin oil) (saturation–aromatic ratio of 0.39 and 4, respectively), with E of 68.9 and 73.6 kcal/mol, respectively [48]. The reactants and products of the cracking process can also be divided into NSOs, C_{14+} unstable concentrated aromatics (Aro–1), C_{14+} stable concentrated aromatics (Aro–2), C_{14+} saturated hydrocarbons, and C_6–C_{13} saturated hydrocarbons [13], their thermal stabilities are also different. The kinetic parameters reported by Behar et al. [13] demonstrated thermal stability similar to that of dodecylbenzene (DDB). The time to achieve 80 % cracking conversion is 245, 235, and 225 Ma, respectively. The initial threshold of the NSOs was the same as that of the aromatics. However, owing to their slightly higher thermal stability, the cracking process path was different from that of the aromatics and saturated hydrocarbons, and the cracking conversion rate increased slowly and rapidly between 240 and 150 Ma. Compared with light hydrocarbons (C_6–C_{13}), C_{14+}-saturated hydrocarbons exhibited weak thermal stability. The cracking and conversion of C_{14+} advanced by 0–2 % at 250–160 Ma, and the difference was as high as 50 % (130 Ma) at a higher thermal evolution level (Fig. 5a). The DY Formation trap oil in the central Sichuan Basin comprises predominantly black shale from the Cambrian Qiongzhusi Formation and a small amount of mud shale from the DY3 and Doushantuo Formations. Organic petrology and regular sterane ternary diagrams confirmed that the biological sources of the Qiongzhusi Formation source rocks were mainly bacteria and algae, and the organic carbon isotope was less than –30 ‰, which belonged to type I organic matter [49]. This indicates a high original hydrogen index and oil generation capacity [50]. High-quality source rocks often produce saturated hydrocarbon-rich oil that is superimposed upon migration. Therefore, Ediacaran oil has characteristics common to marine oil, and it is more reliable to use the thermal cracking experience of marine oil.

The sulfur content in an oil reservoir affected the thermal cracking of the oil. The higher the sulfur content, the lower was the thermal stability. The sulfur content of natural gas in the DY Formation was relatively low (the present-day average content of H_2S was 1.09 %); the sulfur content of the SB revealed by SEM was only approximately 5 % (Fig. 2i), and that revealed by elemental analysis was 4.8 % (n = 105) [38]. Additionally, the current sulfur content was the final result and did not represent the original reservoir oil. However, in general, oil under

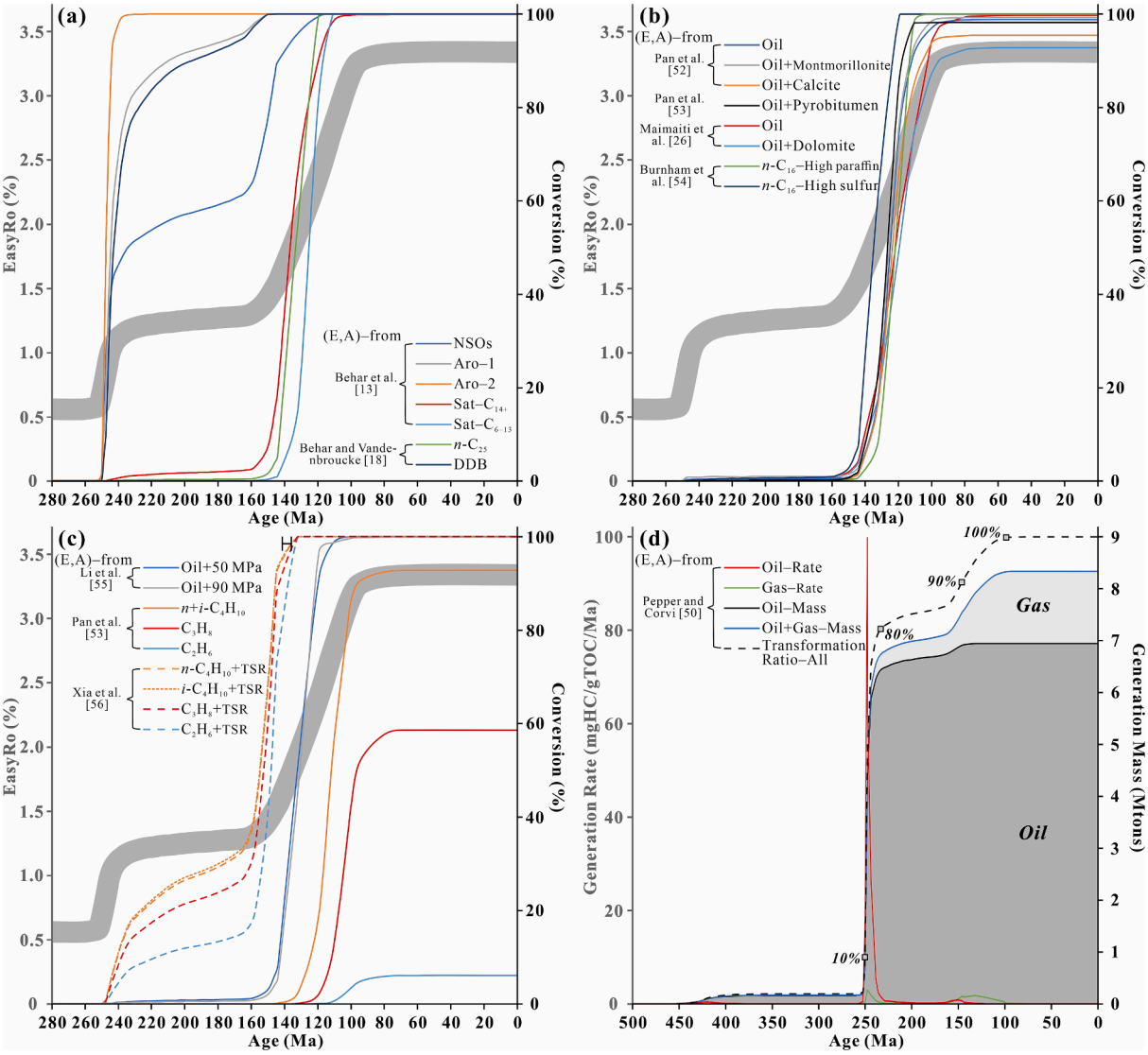

Fig. 5. Kinetic simulation of the DY Formation trap oil cracking (well GS20), central Sichuan Basin. The EasyRo model of the reservoir was based on Sweeney and Burnham [57]. Kinetic data were sourced from Refs [13,18,26,50,52–56].

underground conditions was rich in paraffin with medium or light density, which was caused by migration and fractionation before the thermal evolution of oil, as well as the displacement effect of gas invasion, deasphalting, and volume trapping [51]. Therefore, it can be considered that marine oil with low sulfur content (study area) was more stable than marine oils with high sulfur content; however, the slight difference in E under geological conditions showed a significantly smaller effect than that of TSR, which also required sulfur participation, as discussed in Section 4.3.4.

4.3.2. *Reservoir mineral matrix*

Unlike oil and gas in the source rock, oil cracking in reservoirs had a unique medium condition; i.e., the oil in the reservoir had a higher saturated hydrocarbon content and light components, predominantly owing to the migration effect. Additionally, the oil in the source rocks is closely related to clay minerals, whereas that in the reservoir rocks is mostly related to the reservoir rock type. Based on a gold tube thermal simulation experiment, Pan et al. [52] found that clay minerals (mainly montmorillonite and illite/montmorillonite mixed layers) can accelerate the volume of cracked gas and reduce the E of cracking through acid clay catalysis, which is also closely related to the high specific surface product [58].

However, as an alkaline inhibitor, calcite may hinder further cracking of wet gases during the middle and later stages of oil cracking [25,52]. Maimaiti et al. [26] also demonstrated that dolomite minerals improved the thermal stability of oil to a certain extent, and the average E values of oil and oil + dolomite is 66.22 and 67.80 kcal/mol, respectively. Concurrently, oil cracking in reservoirs is usually affected by the formation of preformed asphalt, including asphaltene formed in the early deasphalting stage and pyrolytic SB formed in the early and middle stages of cracking, although the generation capacity of these substances is limited. Cracking itself plays a catalytic role in oil cracking and may still exist. This effect is reflected by the fact that SB may increase CH_4 production and accelerate wet-gas cracking [53]. Dolomite predominantly developed in the DY Formation carbonate reservoir in the central Sichuan Basin (Fig. 1b). Based on the reported kinetic data analysis, it was also demonstrated that the thermal stability of the DY Formation oil improved to some extent under geological conditions owing to the presence of a dolomite mineral medium in the reservoir (Fig. 5b). Without considering TSR, the cracking conversion rates of crude oil and crude oil + dolomite were 100 % and 93 %, respectively. Therefore, the matrix effect was beneficial for the thermal stability of oil in the dolomite reservoir.

4.3.3. Abnormal pressure

The high formation fluid pressure is closely related to the thermal cracking process of oil in the reservoir [24], where the volume increase is due to the material transformation caused by the primary cracking of liquid hydrocarbons or secondary cracking of wet gas. This is because, at high pressures, the olefin and H_2 contents in the cracking products of laboratory oil are significantly reduced, which is closer to the characteristics of actual natural gas formation [59]. According to kinetic theory, the influence of pressure is complex. Experiments have demonstrated that n-C_{25} thermal cracking rate increases between 12 and 40 MPa and then decreases from 40 to 80 MPa [18,20]. At low temperatures and high pressures, the yields of all the products decreased with increasing pressure. Under high-temperature and low-pressure conditions, an increased pressure generally increases the cracking rate [18,20,60]. The E distribution of oil cracking is narrow [21,55]; therefore, cracking is relatively rapid. In cracking experiments under 50, 100, and 200 MPa, the influence of pressure weakened with a rapid increase in temperature [19]. Hill et al. [15] evaluated the effects of pressure on activation volume. In this process, the reaction mechanism does not change with an increase in pressure as the gas humidity does not change significantly. More importantly, it affects the reaction concentration. In a completely closed system experiment, the generation of wet or dry gas inevitably leads to an abnormally high pressure; therefore, the obtained parameters include and consider the high-pressure suppression effect. Unger et al. [16] observed that the maximum pressure reached 181 MPa, which was directly inferred from the geological conditions. In addition, the oil cracking system was not completely closed under geological conditions, and the abnormally high pressure generated by cracking was properly released. Therefore, the impact of overpressure does exist, but is not extreme or cannot be evaluated. After 250 Ma, the reservoir depth of the DY Formation in the central Sichuan Basin increased rapidly and the hydrostatic pressure increased accordingly. Since 200 Ma, hydrostatic pressure has exceeded 40 MPa. As shown in Fig. 5a, after large-scale oil was filled into the trap at 250 Ma, the most unstable components in the oil began to crack, including Aro–1 and Aro–2. At 200 Ma, nearly 60 % of the NSOs were converted, and the degree of aromatic hydrocarbon conversion was even higher. Because the content of early gas products was very small, the fluid pressure gradually exceeded the hydrostatic pressure after 200 Ma [43].

Li et al. [55] evaluated the influence of pressure on deep oil in the Tarim Basin in Northwest China through the experiments under 50 and 90 MPa and predicted the possible occurrence depth of the oil phase in the Shunbei area. By extrapolating the obtained parameters, the inhibitory effect on oil cracking was found to be insignificant at 90 MPa (Fig. 5c). The cover of the DY gas reservoir is Cambrian Qiongzhusi Formation shale. When the abnormal fluid pressure increased owing to oil cracking in the paleo-oil reservoir, natural gas gradually escaped from the microfracture of the cap rock and the unconformity of the DY Formation at approximately 150 Ma to maintain the relative dynamic balance of energy in the trap [40,61]. The fluid pressure was not as high as would theoretically be expected. Wang et al. [31] also verified this using the paleo-pressure of the inclusion classification in the DY Formation reservoir. In the nearly completely closed CH_4 inclusion with oil cracking SB, the pressure coefficient was 1.54–2.21, recorded by laser Raman shift. However, the actual pressure coefficient of the reservoir with a low sealing property was 1.32–1.79. Although the high pressure still slightly maintained the stability of oil cracking and subsequent wet gas cracking, owing to the rapid and deep burial of the formation and the rapid rise in temperature under the high heat flow, excessive natural gas generated by early cracking was released, which weakened the inhibition of high pressure on the paleo-oil reservoir of the DY Formation in the central Sichuan Basin.

4.3.4. TSR alteration

TSR is a special reaction involving hydrocarbons in a reservoir, including crude oil and sulfate [62–67]. This reaction can occur when the starting temperature and required materials are met. This process consumes crude oil and heavy hydrocarbon gas and produces H_2S, CO_2, and metal sulfides [4,6,62–67]. According to the single group cracking kinetic model of heavy hydrocarbon gas, it can be found that C_2H_6, C_3H_8, and butane (C_4H_{10}) produced by oil cracking have strong thermal stability, and their conversion rate in the actual formation during the secondary thermal cracking process is very low (Fig. 5c), which is inconsistent with the current gas reservoir characteristics of the DY Formation in the central Sichuan Basin. CH_4 was dominant in natural gas from the DY Formation (avg. 90.34 %), whereas C_2H_6 was present in trace amounts (avg. 0.04 %), and C_3H_8 was nearly undetectable (Fig. 6). Based on the kinetic model of heavy hydrocarbon gas cracking under the TSR reaction, the heavy hydrocarbon cracking process was largely promoted by the participation of the TSR, which is consistent with the characteristics of the natural gas components in the current reservoir (Fig. 5c). There is a certain (but no strong quantitative correlation) trend between souring coefficient ($H_2S/(H_2S+\sum C_{1-5})$) and $\delta^{13}C_2H_6$-$\delta^{13}CH_4$, mainly due to the mixing of thermal maturation and TSR. Single thermal maturation and TSR effect on $\delta^{13}C_2H_6$-$\delta^{13}CH_4$ evolution are opposite [67]. From the present-day natural gas composition, the gas reservoir in the study area belongs to the medium–low sulfur gas reservoir, and the H_2S content and souring coefficient are lower than those of typical TSR gas reservoirs [68]. However, there was a small amount of metal sulfide (Fig. 2k–m). Moreover, metal sulfide, SB, and H_2S are rich in $\delta^{34}S$, with average values of 19.4 ‰, 21.88 ‰ and 15.45 ‰, respectively [38,68], indicating that TSR is involved in the formation of metal sulfide and H_2S in gas reservoirs. Notably, the degree of TSR in the study area was weak [4,68]. Because there is no gypsum in the Sinian System, the sulfur sources are supplied from the formation water (Mg^{2+}, avg. 5843.6 mg/L) and the hydrothermal fluid, which are insufficient. Also, the distribution of metal sulfides is very limited [4,68]. In addition, because CH_4 is highly stable and does not participate in the TSR [56,67], whereas heavy hydrocarbon gases (C_2 and C_3) do, the souring coefficient of the gas reservoir will be relatively low (<0.1) [66,67]. Based on these results, the H_2S content (avg. 1.09 %), and souring coefficient (avg. 0.012) in the gas reservoir are low. Therefore, TSR can occur during the entire oil cracking process. The occurrence and selective consumption of TSR leads to the further cracking and alteration of heavy hydrocarbon gas, producing dry gas with a drying coefficient greater than 0.998, including certain amounts of CO_2 and H_2S (Fig. 6) [67]. This was verified by a crude oil simulation experiment in the Tarim Basin and actual natural gas properties of a Mobile Bay reservoir [23,56,69]. Additionally, a fractionation difference in the natural gas isotopes occurs because the ^{12}C bond with lower energy is preferentially consumed in the TSR reaction, resulting in ^{13}C enrichment in the residual gas. Similarly, compared with $\delta^{13}CH_4$, $\delta^{13}C_2H_6$ is significantly greater, which also indicates that the TSR preferentially consumes heavy hydrocarbons.

4.4. Crude oil cracking process under geological conditions

The evolution of the Ediacaran oil and gas system with the Cambrian Qiongzhusi Formation as the major source rock exceeds 541 Ma. The generation and expulsion history of the source rock demonstrates that large-scale hydrocarbon generation began at approximately 250 Ma, and this period was accompanied by a sharp increase in the hydrocarbon generation rate and mass. After approximately 10 million years, the oil and gas generation rate returned to a previously low level, and the total transformation ratio was close to 80 % (Fig. 5d). The large-scale generation and expulsion of oil and gas from the source rock were accompanied by the accumulation of trapped oil, which was also recorded by the Th of the inclusions in the dolomite in the reservoir. The inclusion Th test of 10 samples (n = 260) revealed that the minimum Th was 90–95 °C (Fig. 7). Considering the potential rebalancing of inclusions in carbonate reservoirs, the minimum Th value can be used to limit oil and gas charging times [28]. Additionally, few primary oil-bearing liquid hydrocarbon inclusions were observed under fluorescence, which is also

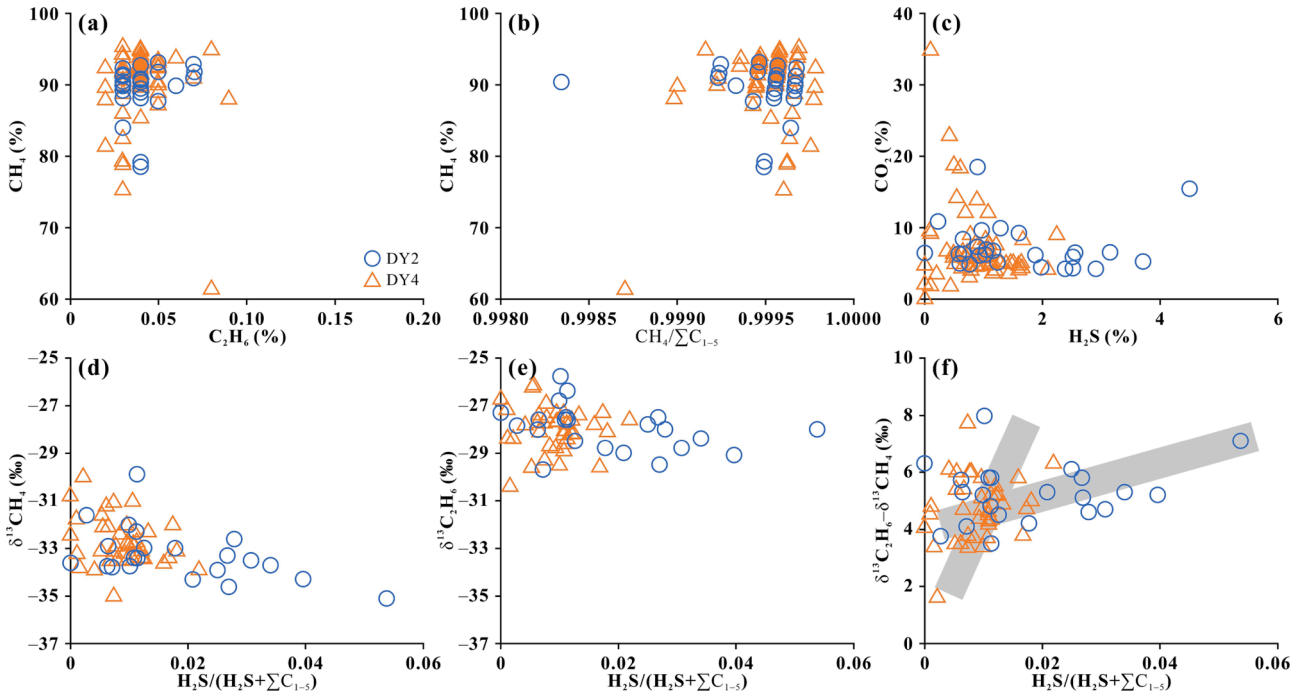

Fig. 6. Natural gas composition and carbon isotope characteristics of the DY Formation, central Sichuan Basin. (Data were sourced from the Oil field and Refs [38,70–72]; Table S2).

the most direct evidence of the existence of paleo-oil reservoirs during the historical period. From 250 to 240 Ma, the Cambrian system was primarily mixed with the Ediacaran source rock for oil expulsion. After the formation of the oil reservoirs, the DY Formation temperature was maintained at approximately 150 °C (EasyRo is approximately 1.2–1.5 %) until approximately 165 Ma.

With the increase in the formation subsidence rate (49.8 m/Ma), the temperature increased rapidly until approximately 100 Ma. The organofacies of the source rock indicate that its gas generation capacity was significantly lower than its oil generation capacity (approximately 1/7) (Fig. 5d). Therefore, the natural gas generated by the source rock dissolves when it enters a pre-existing oil reservoir in succession during the high-temperature evolution stage of the reservoir, and no significant gas invasion occurs. Owing to the formation of oil reservoirs, some of the most unstable components of oil, such as unstable aromatics and NSOs, are the earliest to crack and transform. With further burial depth and an increase in the degree of thermal evolution of the reservoir, the major substances in crude oil, including saturated hydrocarbons, cracked. The cracking products included lighter short-chain saturated hydrocarbons, aromatics, and large amounts of wet gases. The C_1–C_5 wet gases were generated in large quantities at this stage. A large volume of gas can not only dissolve in a small amount in the formation water but also saturate the dissolved gas in the trap oil, weakening the solubility of asphaltene and causing deasphalting and precipitation. These asphaltenes are not heat resistant and constantly precipitate. Because they can also be cracked to generate a small amount of gas, they promote the production of deasphalting, and a small amount of gas is generated to form bitumen with surface pores. Kinetics demonstrates that this process occurred approximately before 125–136 Ma, and the thermal evolution of the reservoir was approximately 1.8–2.2 % (oil conversion rate of 50 %). This time corresponds to the Th (190 °C) recorded by fluid inclusions and is also basically consistent with the Re-Os age (138.6 ± 2.7 Ma) of the reservoir SB reported by Chu et al. [74].

Simultaneously, the extensive residual fluid pressure generated by crude oil cracking was significantly greater than the displacement pressure of the top sealing layer, which caused gas leakage through sealing layer fracture (microfracture) [40,61]. Similarly, a small amount of natural gas can escape through the unconformity between the reservoir and the cap. Excess gas escape maintains a relative energy balance in the trap system, making the actual internal fluid pressure of the reservoir significantly lower than the fluid pressure in a theoretically completely closed system. This was also due to the dynamic dissipation of the SB in all high- and low-structural parts of the current reservoir. Otherwise, because the trapped hydrocarbon-water interface moves down significantly, the high structural part contains almost no SB [75]. The bitumen produced via precipitation at diverse stages under high temperatures and pressures depends on the residual pore space required to produce bitumen with diverse morphologies. The TSR reaction may occur during the entire process; even if the sulfur source supplied by the formation water and thermal fluid is gradually exhausted, the stability of the reactant hydrocarbon gradually increases, and the degree weakens. Thus, TSR can significantly promote crude oil cracking. The formation temperature continued to increase (120–100 Ma) with asphalt precipitation. An increasing amount of wet gas participates in organic–inorganic reactions under high temperatures and TSR alteration. Wet gases such as C_2H_6 are consumed in large amounts, leaving the remaining C_2H_6 with a heavier carbon isotope. Additionally, the cracking of existing bitumen products may generate dry gas, gradually increasing the CH_4 content and forming a dry gas reservoir [76]. The high-viscosity asphalt precipitated by deasphalting at diverse stages, together with bitumen rich in aromatic groups generated by cracking (maintaining the hydrogen balance), was coked to form coke SB with diverse shapes and high reflectivity. This was also reflected in the bitumen with low H/C and O/C atomic ratios (0.478 and 0.165, respectively; Table S3) and high random reflectance (3.39 %, n = 18, [39]). After 100 Ma (Late Yanshanian–Himalayan), the Sichuan Basin was uplifted and eroded, and the natural gas in the gas reservoir partially escaped along the unconformity interface, whereas the dissolved natural gas in the formation water was released as a supplement, forming the current pattern of the Ediacaran DY Formation dry gas reservoir (Fig. 8).

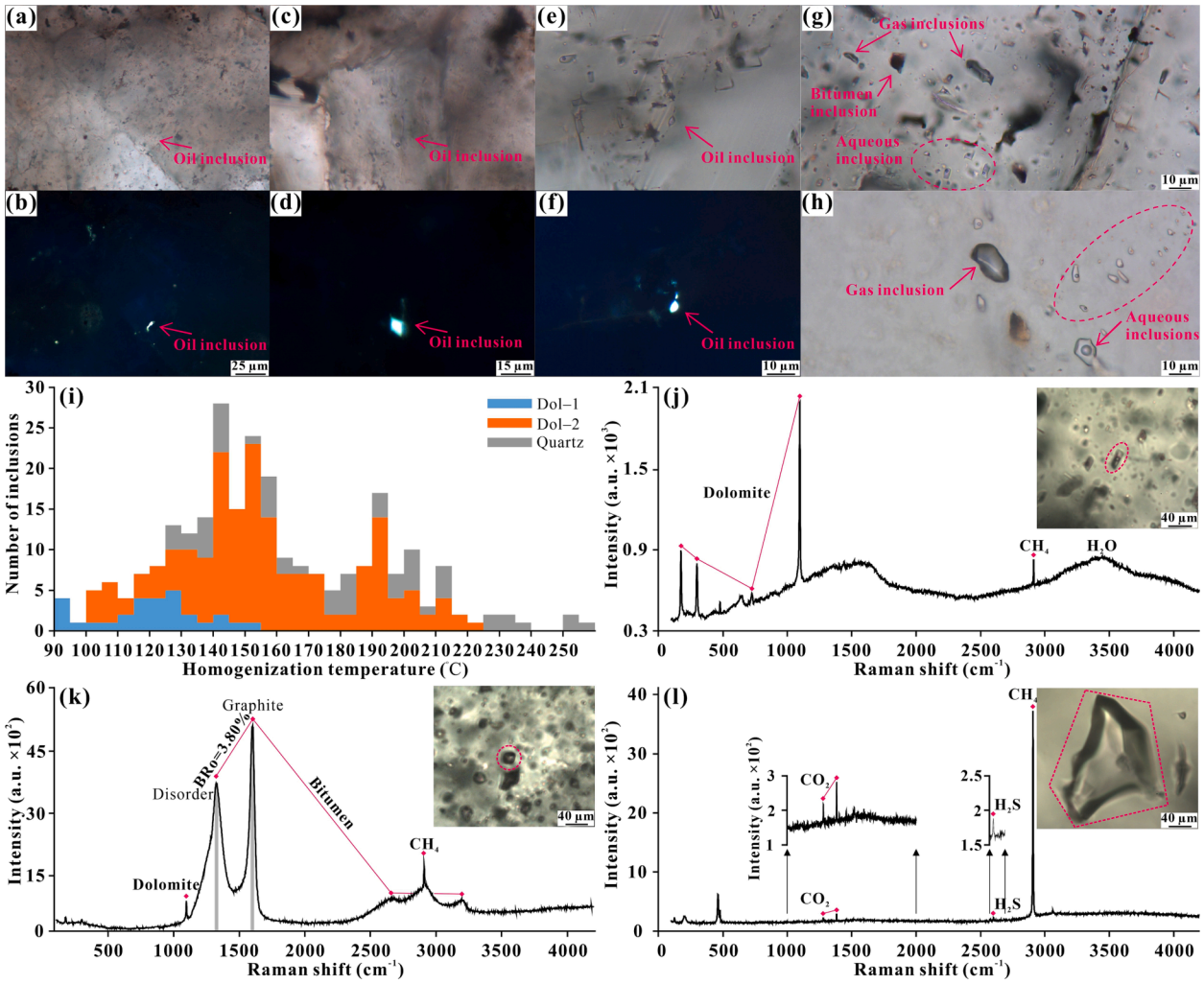

Fig. 7. Fluid inclusion testing of the DY Formation reservoir, central Sichuan Basin. (a–b) Plane-polarized light and UV-excited fluorescence depict a small amount of liquid hydrocarbon oil inclusions, PS1, 7281.43 m; (c–f) liquid hydrocarbon oil inclusions with light blue to yellow white fluorescence, GS20, 5194.33 m; (g–h) dark gray gas inclusions, black bitumen inclusions, and colorless gray hydrocarbon aqueous inclusions under plane-polarized light, PS1, 7281.43 m (g) and 7284.74 m (h); (i) homogenization temperature of fluid inclusions from diverse host minerals; (j) laser Raman of CH_4 dominated gas-aqueous two-phase inclusions, PS1, 7281.43 m; (k) Laser Raman of pure CH_4 gas inclusions containing bitumen, ZJ2, 6558.32 m, the equivalent bitumen reflectance (BRo) is computed based on the intensity of Disorder and Graphite peaks [73]; (l) laser Raman of CH_4 gas inclusions with trace amounts of CO_2 and H_2S, GS124, 5566.9 m. (For interpretation of the references to color in this figure legend, the reader is referred to the web version of this article.)

5. Conclusions

This study was based on the Ediacaran natural gas reservoir in the Sichuan Basin, China. Based on the characteristics of reservoir minerals, natural gas, and residual SB, combined with fluid inclusion analysis, U–Pb dating, basin simulation, and crude oil cracking kinetic technology, forward and inversion processes were combined to restore the complete process of oil cracking under geological conditions. The following conclusions were drawn:

(1) The large-scale distribution of SB in the reservoir, a small number of primary oil-bearing liquid hydrocarbon inclusions, and SB-CH_4 gas inclusions are the most direct evidence of Ediacaran gas reservoir formation in the central Sichuan Basin from the cracking of the paleo-oil reservoir.

(2) Under geological conditions, several factors affect trapped oil cracking; however, the temperature evolution of the reservoir is decisive, followed by the composition type of crude oil, TSR reaction, formation pressure, and other factors. The wet gases generated in the early stage partially dissipated under high residual pressure, thereby reducing the inhibitory effect of high pressure on cracking. The escape of early gas products and significant promotion of the TSR reaction to wet gas cracking formed a CH_4-rich dry gas reservoir with a high drying coefficient in the present-day reservoir.

(3) The cracking process of crude oil from the Ediacaran paleo-reservoir can be divided into four stages: cracking and transformation of the most unstable components, including NSOs and aromatics, and thermal cracking of the major components in the crude oil. After a large amount of produced natural gas reaches the limit of dissolution in the oil, it first causes deasphalting of the trap oil and then breaks through the sealing layer or unconformity surface to achieve a dynamic balance of energy. The TSR reaction is then involved in further thermal cracking of the residual oil and wet gases. Subsequently, the bitumen generated in diverse stages coked and the gas components in the reservoir were finalized.

CRediT authorship contribution statement

Yishu Li: . Guangdi Liu: Funding acquisition, Methodology, Writing – review & editing. **Zezhang Song:** Writing – review & editing.

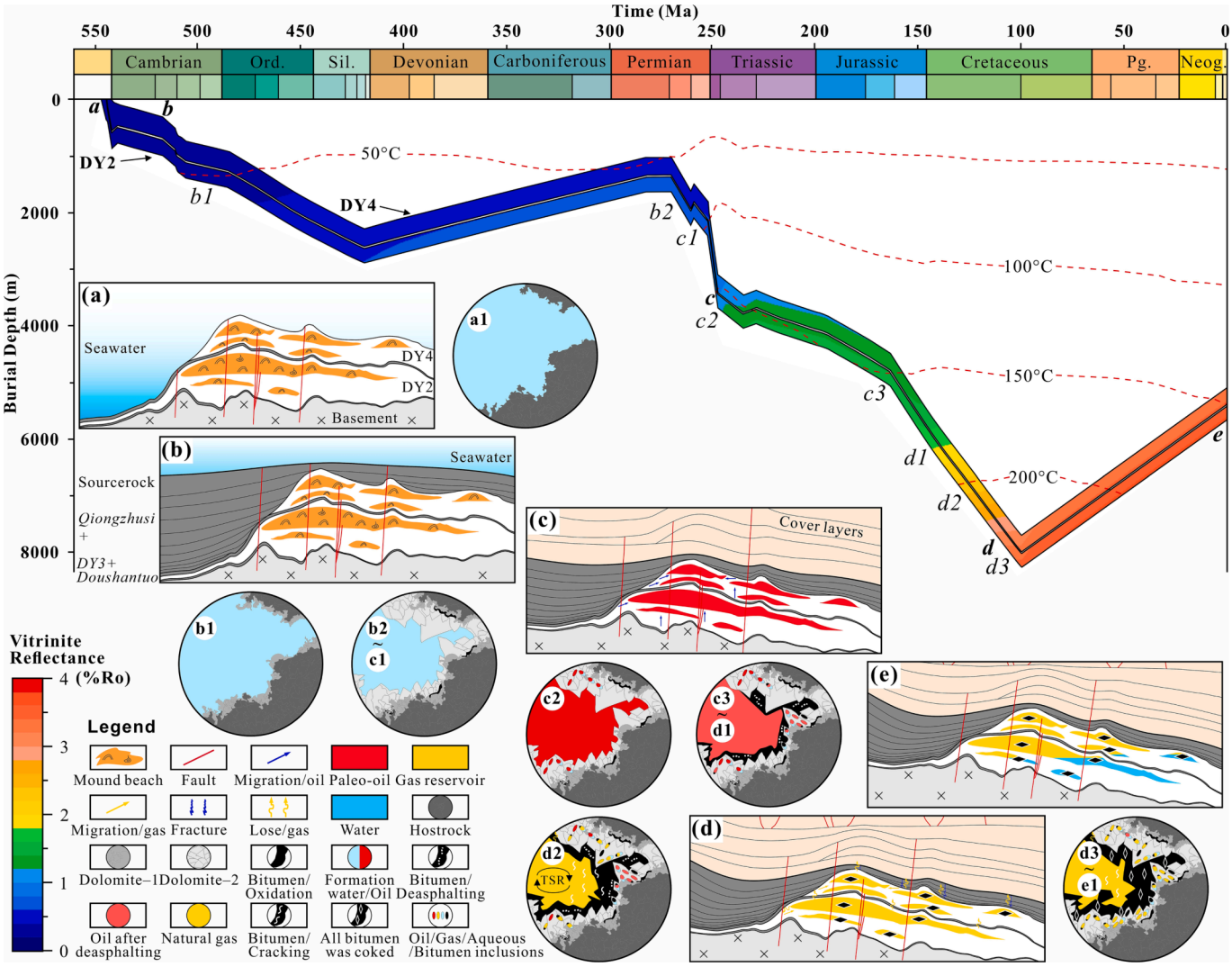

Fig. 8. Thermal cracking model of crude oil from the DY Formation paleo-oil reservoir in the central Sichuan Basin.

Mingliang Sun: Writing – review & editing. **Xingwang Tian:** Resources. **Dailing Yang:** Resources. **Lianqiang Zhu:** Investigation.

Declaration of competing interest

The authors declare that they have no known competing financial interests or personal relationships that could have appeared to influence the work reported in this paper.

Data availability

Data will be made available on request.

Acknowledgements

This research was supported by the National Key R&D Program of China (Grant No. 2017YFC0603106) and National Natural Science Foundation of China (Grant No. 42272161). We sincerely thank the Research Institute of Exploration and Development, PetroChina Southwest Oil & Gas Field Company for providing samples and data. We thank Yang Xiao for his help in dolomite U–Pb dating test, and Dr. Jian Ma for her help in the fluid inclusion test. We sincerely thank to editors and reviewers for their detailed and constructive comments that significantly improved the manuscript.

Appendix A. Supplementary data

Supplementary data to this article can be found online at https://doi.org/10.1016/j.fuel.2024.131063.

References

[1] Isaksen GH. Central North Sea hydrocarbon systems: Generation, migration, entrapment, and thermal degradation of oil and gas. AAPG Bull 2004;88:1545–72. https://doi.org/10.1306/06300403048.
[2] Wang YP, Zhang SC, Wang FY, Wang ZY, Zhao CY, Wang HJ, et al. Thermal cracking history by laboratory kinetic simulation of Paleozoic oil in eastern Tarim Basin, NW China, implications for the occurrence of residual oil reservoirs. Org Geochem 2006;37:1803–15. https://doi.org/10.1016/j.orggeochem.2006.07.010.
[3] Mancini EA, Li P, Goddard DA, Ramirez V, Talukdar SC. Mesozoic (Upper Jurassic-Lower Cretaceous) deep gas reservoir play, central and eastern Gulf coastal plain. AAPG Bull 2008;92:283–308. https://doi.org/10.1306/11120707084.
[4] Zhu GY, Wang TS, Xie ZY, Xie BH, Liu KY. Giant gas discovery in the Precambrian deeply buried reservoirs in the Sichuan Basin, China: implications for gas exploration in old cratonic basins. Precambr Res 2015;262:45–66. https://doi.org/10.1016/j.precamres.2015.02.023.
[5] Zhu GY, Li JF, Zhang ZY, Wang M, Xue N, He T, et al. Stability and cracking threshold depth of crude oil in 8000 m ultra-deep reservoir in the Tarim Basin. Fuel 2020;282:118777. https://doi.org/10.1016/j.fuel.2020.118777.
[6] Liu QY, Jin ZJ, Li HL, Wu XQ, Tao XW, Zhu DY, et al. Geochemistry characteristics and genetic types of natural gas in central part of the Tarim Basin. NW China Marine and Petroleum Geology 2018;89:91–105. https://doi.org/10.1016/j.marpetgeo.2017.05.002.
[7] Song YF, Chen Y, Wang M, MacInnis MS, Ni R, Zhang H, et al. In-situ cracking of oil into gas in reservoirs identified by fluid inclusion analysis: Theoretical model and

case study. Mar Pet Geol 2023;147:105959. https://doi.org/10.1016/j.marpetgeo.2022.105959.
[8] Tissot BP, Welte DH. Petroleum formation and occurrence. second revised and enlarged. Berlin, Heidelberg, New York, Tokyo: Springer-Verlag; 1984.
[9] Blanc P, Connan J. Preservation, degradation, and destruction of trapped oil. AAPG Mem 1994;60:237–47. https://doi.org/10.1306/M60585C14.
[10] Evans CR, Rogers MA, Bailey NJL. Evolution and alteration of petroleum in western Canada. Chem Geol 1971;8:147–70. https://doi.org/10.1016/0009-2541(71)90002-7.
[11] Rogers MA, McAlary JD, Bailey NJL. Significance of reservoir bitumens to thermal-maturation studies, western Canada Basin. AAPG Bull 1974;58:1806–24. https://doi.org/10.1306/83D919B6-16C7-11D7-8645000102C1865D.
[12] Behar F, Kressmann S, Rudkiewicz JL, Vandenbroucke M. Experimental simulation in a confined system and kinetic modelling of kerogen and oil cracking. Org Geochem 1992;19:173–89. https://doi.org/10.1016/0146-6380(92)90035-V.
[13] Behar F, Lorant F, Mazeas L. Elaboration of a new compositional kinetic schema for oil cracking. Org Geochem 2008;39:764–82. https://doi.org/10.1016/j.orggeochem.2008.03.007.
[14] Takach NE, Barker C, Kemp MK. Stability of natural gas in the deep subsurface: Thermodynamic calculation of equilibrium compositions. AAPG Bull 1987;71:322–33. https://doi.org/10.1306/94886E8E-1704-11D7-8645000102C1865D.
[15] Hill RJ, Tang YC, Kaplan IR. Insights into oil cracking based on laboratory experiments. Org Geochem 2003;34:1651–72. https://doi.org/10.1016/S0146-6380(03)00173-6.
[16] Ungerer P, Behar F, Villalba M, Heum OR, Audibert A. Kinetic modelling of oil cracking. Org Geochem 1988;13:857–68. https://doi.org/10.1016/0146-6380(88)90238-0.
[17] Pepper AS, Dodd TA. Simple kinetic models of petroleum formation. Part II: oil-gas cracking. Mar Pet Geol 1995;12:321–40. https://doi.org/10.1016/0264-8172(95)98382-F.
[18] Behar F, Vandenbroucke M. Experimental determination of the rate constants of the n-C_{25} thermal cracking at 120, 400, and 800 bar: Implications for high-pressure/high-temperature prospects. Energy Fuel 1996;10:932–40. https://doi.org/10.1021/ef9600366.
[19] Zhao WZ, Wang ZY, Zhang SC, Wang HJ. Cracking conditions of crude oil under different geological environments. Science in China: Earth Sciences 2008;51:77–83. https://doi.org/10.1007/s11430-008-5002-4.
[20] Fabuss BM, Smith JO, Lait RI, Borsanyi AS, Satterfield CN. Rapid thermal cracking of n-Hexadecane at elevated pressures. Ind Eng Chem Process Des Dev 1962;1:293–9. https://doi.org/10.1021/i260004a011.
[21] Waples DW. The kinetics of in-reservoir oil destruction and gas formation: constraints from experimental and empirical data, and from thermodynamics. Org Geochem 2000;31:553–75. https://doi.org/10.1016/S0146-6380(00)00023-1.
[22] Vitzthum VB, Michels R, Scacchi G, Marquaire PM, Dessort D, Pradier B, et al. Kinetic effect of alkylaromatics on the thermal stability of hydrocarbons under geological conditions. Org Geochem 2004;35:3–31. https://doi.org/10.1016/j.orggeochem.2003.06.001.
[23] Zhang SC, Zhu GY, He K. The effects of thermochemical sulfate reduction on occurrence of oil-cracking gas and reformation of deep carbonate reservoir and the interaction mechanisms. Acta Petrol Sin 2011;27:809–26. in Chinese.
[24] Uguna CN, Carr AD, Snape CE, Meredith W. Retardation of oil cracking to gas and pressure induced combination reactions to account for viscous oil in deep petroleum basins: Evidence from oil and n-hexadecane pyrolysis at water pressures up to 900 bar. Org Geochem 2016;97:61–73. https://doi.org/10.1016/j.orggeochem.2016.04.007.
[25] He M, Wang ZY, Moldowan MJ, Peters K. Insights into catalytic effects of clay minerals on hydrocarbon composition of generated liquid products during oil cracking from laboratory pyrolysis experiments. Org Geochem 2022;163:104331. https://doi.org/10.1016/j.orggeochem.2021.104331.
[26] Maimaiti A, Wang Q, Hao F, Yang XZ, Zhang HZ, Tian JQ. Oil pyrolysis with carbonate minerals: Implications for the thermal stability of deep crude oil. Mar Pet Geol 2022;146:105929. https://doi.org/10.1016/j.marpetgeo.2022.105929.
[27] Xu CC, Shen P, Yang YM, Zhao LZ, Luo B, Wen L, et al. New understandings and potential of Sinian-Lower Paleozoic natural gas exploration in the central Sichuan paleo-uplift of the Sichuan Basin. Nat Gas Ind 2021;8:105–13. https://doi.org/10.1016/j.ngib.2020.07.007.
[28] Bourdet J, Pironon J, Levresse G, Tritlla J. Petroleum accumulation and leakage in a deeply buried carbonate reservoir, Nispero field (Mexico). Mar Pet Geol 2010;27:126–42. https://doi.org/10.1016/j.marpetgeo.2009.07.003.
[29] Cheng T, Zhao JX, Feng YX, Pan WQ, Liu DY. In-situ LA-MC-ICPMS U-Pb dating method for low-uranium carbonate minerals. Chin Sci Bull 2020;65:150–4. https://doi.org/10.1360/TB-2019-0355.
[30] Qiao RZ, Chen ZH. Petroleum phase evolution at high temperature: A combined study of oil cracking experiment and deep oil in Dongying Depression, eastern China. Fuel 2022;326:124978. https://doi.org/10.1016/j.fuel.2022.124978.
[31] Wang X, Tian H, Xiao XM, Liu DH, Min YS, Li TF, et al. Methane-dominated gaseous inclusions in the Sinian carbonate reservoirs in central Sichuan Basin and their implications for natural gas accumulation. Mar Pet Geol 2021;125:104871. https://doi.org/10.1016/j.marpetgeo.2020.104871.
[32] Liu B. Fluid entrapment thermodynamics. Beijing: Geological Publishing House; 1999.
[33] Lu WJ, Chou IM, Burruss RC, Song YC. A unified equation for calculating methane vapor pressures in the CH_4–H_2O system with measured Raman shifts. Geochim Cosmochim Acta 2007;71:3969–78. https://doi.org/10.1016/j.gca.2007.06.004.
[34] Duan ZH, Møller N, Weare JH. An equation of state for the CH_4-CO_2-H_2O system: I. Pure systems from 0 to 1000°C and 0 to 8000 bar. Geochim Cosmochim Acta 1992;56:2605–17. https://doi.org/10.1016/0016-7037(92)90347-L.
[35] Paton C, Hellstrom J, Paul B, Woodhead J, Hergt J. Iolite: Freeware for the visualisation and processing of mass spectrometric data. J Anal At Spectrom 2011;26:2508–18. https://doi.org/10.1039/C1JA10172B.
[36] Qiu NS, Chang J, Zhu CQ, Liu W, Zuo YH, Xu W, et al. Thermal regime of sedimentary basins in the Tarim, Upper Yangtze and North China Cratons. China Earth-Science Reviews 2022;224:103884. https://doi.org/10.1016/j.earscirev.2021.103884.
[37] Huang H, Huyskens MH, Yin QZ, Cawood PA, Hou MC, Yang JH, et al. Eruptive tempo of Emeishan large igneous province, southwestern China and northern Vietnam: Relations to biotic crises and paleoclimate changes around the Guadalupian-Lopingian boundary. Geology 2022;50:1083–107. https://doi.org/10.1130/G50183.1.
[38] Zhang PW, Liu GD, Cai CF, Li MJ, Chen RQ, Gao P, et al. Alteration of solid bitumen by hydrothermal heating and thermochemical sulfate reduction in the Ediacaran and Cambrian dolomite reservoirs in the Central Sichuan Basin. SW China Precambrian Research 2019;321:277–302. https://doi.org/10.1016/j.precamres.2018.12.014.
[39] Gao P, Liu GD, Lash GG, Li BY, Yan DT, Chen C. Occurrences and origin of reservoir solid bitumen in Sinian Dengying Formation dolomites of the Sichuan Basin, SW China. Int J Coal Geol 2018;200:135–52. https://doi.org/10.1016/j.coal.2018.11.001.
[40] Li Q, Liu GD, Song ZZ, Sun ML, Cao YS, Zhu LQ, et al. Analysis on preservation effectiveness of lithologic gas reservoirs in north slope of central Sichuan paleo-uplift: Case study of the second member of the Dengying Formation in Well Pengtan-1. Nat Gas Geosci 2022;33:1276–85. in Chinese.
[41] Su A, Chen HH, Feng YX, Zhao JX, Wang ZC. Paleo fluid system change from deep burial to exhumation of the Precambrian petroleum reservoirs in the Sichuan Basin, China: Evidence from P-T-X records. Mar Pet Geol 2023;155:106404. https://doi.org/10.1016/j.marpetgeo.2023.106404.
[42] Barker C. Calculated volume and pressure changes during the thermal cracking of oil to gas in reservoirs. AAPG Bull 1990;74:1254–61. https://doi.org/10.1306/0C9B247F-1710-11D7-8645000102C1865D.
[43] Liu W, Qiu NS, Xu QC, Liu YF. Precambrian temperature and pressure system of Gaoshiti-Moxi block in the central paleo-uplift of Sichuan Basin, southwest China. Precambr Res 2018;313:91–108. https://doi.org/10.1016/j.precamres.2018.05.028.
[44] Claypool GE, Mancini EA. Geochemical relationships of petroleum in Mesozoic reservoirs to carbonate source rocks of Jurassic Smackover Formation. Southwest Alabama AAPG Bulletin 1989;73:904–24. https://doi.org/10.1306/44B4A28F-170A-11D7-8645000102C1865D.
[45] McCain WD, Bridges B. Volatile oils and retrograde gases-What's the difference? Pet Eng Int 1994;66:35–6.
[46] Hunt J. Petroleum geology and geochemistry. 2nd ed. New York: Freeman; 1996.
[47] Ma AL. Kinetics of oil-cracking for different types of marine oils from Tahe Oilfield, Tarim Basin, NW China. J Nat Gas Geosci 2016;1:35–43. https://doi.org/10.1016/j.jnggs.2016.03.001.
[48] Schenk HJ, Primio RD, Horsfield B. The conversion of oil into gas in petroleum reservoirs. Part 1: Comparative kinetic investigation of gas generation from crude oils of lacustrine, marine and fluviodeltaic origin by programmed-temperature closed-system pyrolysis. Org Geochem 1997;26:467–81. https://doi.org/10.1016/S0146-6380(97)00024-7.
[49] Li YS, Liu GD, Song ZZ, Zhang BJ, Sun ML, Tian XW, et al. Organic matter enrichment due to high primary productivity in the deep-water shelf: Insights from the lower Cambrian Qiongzhusi shales of the central Sichuan Basin, SW China. J Asian Earth Sci 2022;239:105417. https://doi.org/10.1016/j.jseaes.2022.105417.
[50] Pepper AS, Corvi PJ. Simple kinetic models of petroleum formation. Part I: oil and gas generation from kerogen. Mar Pet Geol 1995;12:291–319. https://doi.org/10.1016/0264-8172(95)98381-E.
[51] Horsfield B, Schenk HJ, Mills N, Welte DH. An investigation of the in-reservoir conversion of oil to gas: compositional and kinetic findings from closed-system programmed-temperature pyrolysis. Org Geochem 1992;19:191–204. https://doi.org/10.1016/0146-6380(92)90036-W.
[52] Pan CC, Jiang LL, Liu JZ, Zhang SC, Zhu GY. The effects of calcite and montmorillonite on oil cracking in confined pyrolysis experiments. Org Geochem 2010;41:611–26. https://doi.org/10.1016/j.orggeochem.2010.04.011.
[53] Pan CC, Jiang LL, Liu JZ, Zhang SC, Zhu GY. The effects of pyrobitumen on oil cracking in confined pyrolysis experiments. Org Geochem 2012;45:29–47. https://doi.org/10.1016/j.orggeochem.2012.01.008.
[54] Burnham AK, Gregg HR, Ward RL, Knauss KG. Decomposition kinetics and mechanism of n-hexadecane-l,2–^{13}C2 and dodec-l-ene-l,2–^{13}C2 doped in petroleum and n-hexadecane. Geochim Cosmochim Acta 1997;61:3725–37. https://doi.org/10.1016/S0016-7037(97)00182-8.
[55] Li HL, Ma AL, Cai XY, Lin HX, Li JJ, Liu JZ, et al. Kinetics of oil-cracking of ultra-deep Ordovician oil in the North Shuntuoguole area of Tarim Basin and its geological implications. Pet Geol Exp 2021;43:818–25. in Chinese.
[56] Xia XY, Ellis GS, Ma QS, Tang YC. Compositional and stable carbon isotopic fractionation during non-autocatalytic thermochemical sulfate reduction by gaseous hydrocarbons. Geochim Cosmochim Acta 2014;139:472–86. https://doi.org/10.1016/j.gca.2014.05.004.
[57] Sweeney JJ, Burnham AK. Evaluation of a simple model of vitrinite reflectance based on chemical kinetics1. AAPG Bull 1990;74:1559–70. https://doi.org/10.1306/0C9B251F-1710-11D7-8645000102C1865D.

[58] Ranjbar M. Influence of reservoir rock composition on crude oil pyrolysis and combustion. J Anal Appl Pyrol 1993;27:87–95. https://doi.org/10.1016/0165-2370(93)80024-T.
[59] Wang ZP, Fu XT, Lu SF, Qu JY. An analogue experiment of gas generating by crude oil cracking, characters of products and its significance. Nat Gas Ind 2001;21:12–5. in Chinese.
[60] Jackson KJ, Burnham AK, Braun RL, Knauss KG. Temperature and pressure dependence of n-hexadecane cracking. Org Geochem 1995;23:941–53. https://doi.org/10.1016/0146-6380(95)00068-2.
[61] Hao F, Guo TL, Zhu YM, Cai XY, Zou HY, Li PP. Evidence for multiple stages of oil cracking and thermochemical sulfate reduction in the Puguang Gas Field, Sichuan Basin, China. AAPG Bull 2008;92:611–37. https://doi.org/10.1306/01210807090.
[62] Liu QY, Worden RH, Jin ZJ, Liu WH, Li J, Gao B, et al. Thermochemical sulphate reduction (TSR) versus maturation and their effects on hydrogen stable isotopes of very dry alkane gases. Geochim Cosmochim Acta 2014;137:208–20. https://doi.org/10.1016/j.gca.2014.03.013.
[63] Hao F, Zhang XF, Wang CW, Li PP, Guo TL, Zou HY, et al. The fate of CO_2 derived from thermochemical sulfate reduction (TSR) and effect of TSR on carbonate porosity and permeability, Sichuan Basin. China Earth-Science Reviews 2015;141:154–77. https://doi.org/10.1016/j.earscirev.2014.12.001.
[64] Liu QY, Zhu DY, Jin ZJ, Liu CY, Zhang DW, He ZL, et al. Coupled alteration of hydrothermal fluids and thermal sulfate reduction (TSR) in ancient dolomite reservoirs–An example from Sinian Dengying Formation in Sichuan Basin, southern China. Precambr Res 2016;285:39–57. https://doi.org/10.1016/j.precamres.2016.09.006.
[65] Liu QY, Peng WL, Meng QQ, Zhu DY, Jin ZJ, Wu XQ. Fractionation of carbon and hydrogen isotopes of TSR-altered gas products under closed system pyrolysis. Sci Rep 2020;10:12921.
[66] Wu XQ, Liu QY, Chen YB, Zhai CB, Ni CH, Jun Y. Constraints of molecular and stable isotopic compositions on the origin of natural gas from Middle Triassic reservoirs in the Chuanxi large gas field, Sichuan Basin, SW China. J Asian Earth Sci 2020;204:104589. https://doi.org/10.1016/j.jseaes.2020.104589.
[67] Liu QY, Worden RH, Jin ZJ, Liu WH, Li J, Gao B, et al. TSR versus non-TSR processes and their impact on gas geochemistry and carbon stable isotopes in Carboniferous, Permian and Lower Triassic marine carbonate gas reservoirs in the Eastern Sichuan Basin. China Geochimica et Cosmochimica Acta 2013;100:96–115. https://doi.org/10.1016/j.gca.2012.09.039.
[68] Liu Q, Lu XS, Fan JJ, Liu SB, Ma XZ, Dai BK, et al. Evidence and controlling factors of thermochemical sulfate reduction in the Sinian gas reservoirs. Sichuan Basin Natural Gas Geoscience 2022;33:929–43. in Chinese.
[69] Xia XY. Kinetics of gaseous hydrocarbon generation with constraints of natural gas composition from the Barnett Shale. Org Geochem 2014;74:143–9. https://doi.org/10.1016/j.orggeochem.2014.02.009.
[70] Xie ZY, Wei GQ, Li J, Xu L, Zhang L, Li J, et al. Geochemical characteristics and accumulation pattern of gas reservoirs of the Sinian-Permian in central Sichuan uplift zone. Sichuan Basin China Petroleum Exploration 2021;26:50–67. in Chinese.
[71] Xie ZY, Li J, Yang CL, Tian XW, Zhang L, Li J, et al. Geochemical characteristics of Sinian-Cambrian natural gas in central Sichuan paleo-uplift and exploration potential of Taihe gas area. Nat Gas Ind 2021;41:1–14. in Chinese.
[72] Wei GQ, Xie ZY, Yang Y, Li J, Yang W, Zhao LZ, et al. Formation conditions of Sinian-Cambrian large lithologic gas reservoirs in the north slope area of central Sichuan Basin. SW China Petroleum Exploration and Development 2022;49:963–76. https://doi.org/10.1016/S1876-3804(22)60325-2.
[73] Wang ML, Xiao XM, Wei Q, Zhou Q. Thermal maturation of solid bitumen in shale as revealed by Raman spectroscopy. Nat Gas Geosci 2015;26:1712–8. in Chinese.
[74] Chu ZY, Wang MJ, Liu DW, Liu JJ, Guo JH, Zhang H. Re-Os dating of gas accumulation in Upper Ediacaran to Lower Cambrian dolostone reservoirs, Central Sichuan Basin. China Chemical Geology 2023;620:121342. https://doi.org/10.1016/j.chemgeo.2023.121342.
[75] Huang WM, Xu QK, Liu SG, Zeng DF, Zheng RC, Ma WX. Coupling relationship between oil & gas accumulation process and reservoir bitumen of marine system: Taking Sichuan Basin as an example. Geol Sci Technol Information 2015;34:159–68. in Chinese.
[76] Xiao XM, Fang F, Wilkins RWT, Song ZG. Origin and gas potential of pyrobitumen in the Upper Proterozoic strata from the Middle Paleo-Uplift of the Sichuan Basin. China Int J Coal Geol 2007;70:264–76. https://doi.org/10.1016/j.coal.2006.03.007.